

# A DESIGN FOR CONTINUOUSLY VARIABLE TRANSMISSION CONSISTING OF LINKS, CRANKS, CAMS, AND FREEWHEELS

Toshihiro Yukawa\*

## Abstract

This paper describes a continuously variable transmission (CVT) consisting of links, cranks, cams, and freewheels. Generally, power transmission mechanism such as the CVT has been used in vehicles or construction machineries, *etc.* Conventional CVTs are mainly classified as belt-type or toroidal-type CVTs based on the difference between their fundamental conduction mechanisms. The proposed CVT consists of closed-loop linkages, three-dimensional cams, and irreversible mechanisms such as freewheels, and it does not depend on any frictional conduction forces in the mechanism. This CVT can provide high functions that create no noise, is durable, and offers high transmission efficiency. All units, in which each slider-crank mechanism is installed, are connected in parallel at both the input and output shafts in the CVT. On the output side, each crankshaft in each unit is connected mechanically at a common output axis through freewheels. The main purpose of this paper is to design the outer shape of the cam inside the CVT unit, design it for each gear ratio, and then build a CVT in which multiple units are arranged in parallel. In this CVT, the continuous rotation input from the input shaft can continuously rotate the output shaft regardless of the arbitrary gear ratio, and the output shaft rotates in proportion as the rotation speed of the input shaft in relation to the arbitrary gear ratio. In this paper, we derive a mathematical linkage model for the slider-crank mechanism installed in the CVT. In particular, we analyse the geometry of the relationship between the link mechanisms and the three-dimensional cam. As this conduction mechanism is not composed of frictional components, it provides high transmission efficiency.

## Key Words

Continuously variable transmission, four-bar linkage, slider-crank mechanism, freewheel, one-way clutch, cam, frictional force

\* Iwate University, 4-3-5 Ueda, Morioka, Iwate, 020-8551, Japan;  
e-mail: yukawat@iwate-u.ac.jp

Corresponding author: Toshihiro Yukawa  
Recommended by Dr. Dong W. Kim  
(DOI: 10.2316/J.2022.201-0287)

## 1. Introduction

### 1.1 Historical Background of Studies on Mechatronics Related to Sustainable Development Goals

From the viewpoint of sustainable development goals, wind power generation using natural energy has been reviewed in terms of its efficiency in recent years. Many studies on wind power generation, turbine, and electric generator used in wind power generators and motor control method of generators have been actively developed. As for the study of the wind turbine generator, Shi *et al.* have studied the induction principle and fault characteristics of the transmission system gear fault information in the stator current signal based on the motion equation of the asynchronous motor [1]. Si *et al.* have analysed the structure and vibration characteristics of planetary gear, built the wind turbine test, and analysed the results of fault experiments [2]. Boufounas *et al.* have presented a robust multivariable control design for a variable-speed variable-pitch wind turbine [3]. Farnaz *et al.* have compared the performance of closed-loop state estimator with a Kalman filter implemented for the same purpose. The input voltage to the motor and the speed output of the motor were the input to the state estimator, while the estimated torque was the output of the estimator, which was used for closed-loop torque control of the DC motor [4].

To increase the efficiency in the power generation, we propose a new type of mechanical system where a continuously variable transmission (CVT) is installed. As our developed CVT is able to change the gear ratio continuously, it is able to transfer rotational energy from wind force to the turbine or the electric generator with high efficiency.

### 1.2 Conventional Continuously Variable Transmissions

Conventional CVTs are mainly classified as belt-type or toroidal CVTs. Basically, each CVT is composed of frictional conduction mechanism. The belt-type CVT has a mechanism which transmits power and torque with V-belt and pulley. The gear ration is changed continuously by

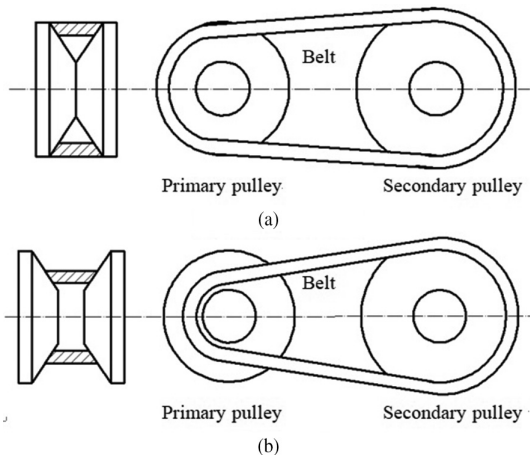


Figure 1. The belt-type CVT.

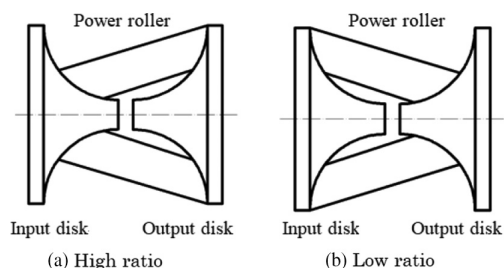


Figure 2. The toroidal CVT.

controlling the effective diameter of the pulley to contact with the V-belt in order to transmit the power and torque, as shown in Fig. 1. Figure 1(a) shows the high gear ratio state, and Fig. 1(b) shows the low gear ratio state. The toroidal CVT has a mechanism where a power roller is placed between the input and output disks, as shown in Fig. 2. The contact points between both input and output disks and the power rollers are changed as the inclination corner of the power rollers is changed along the rotation axis by another exterior force in order to change the gear ratio. Figure 2(a) shows a low-speed rotation state of the output shaft, and Fig. 2(b) shows a high-speed rotation state of the output shaft.

### 1.3 Historical Background of Continuously Variable Transmission

Currently, several kinds of CVTs are installed mainly in vehicles, but it is expected that the applications of CVTs will be expanded to machine tools, generators, large vehicles, and construction machines and that CVT technology will be improved in the future. Various other types of CVTs have been proposed by many researchers. For instance, the new CVT which is small and lightweight attributes allows to be used in human-powered transport devices such as bicycles [5]. Many studies of CVTs that are mounted on hybrid vehicles [6], [7] and new types of CVTs such as the elastic conservative transmission [8] have already been done. Some studies of the application techniques related to CVTs and study examples [9] of mounting CVTs on

wheeled robots have also been done. A. Afrabandpey *et al.* have studied an analytical model of ball CVT behaviour and performance, based on the existing model of the half-toroidal traction drive [10]. Pohl *et al.* have analysed the configuration of a spherical traction drive in the CVT and the infinitely variable transmission [11]. Belter *et al.* have developed a passively adaptive rotary-to-linear CVT with the ability to passively change gear ratio as a function of the output load [12]. Saribay *et al.* have investigated the kinematics, gear tooth load capacity, bearing load capacity, and mesh efficiency of the pericyclic mechanical transmission system with a high reduction ratio, high tooth contact ratio, and nutating and rotating gear mechanism which incorporates meshing conjugate face-gear pairs [13]. You *et al.* have proposed a parameter matching design method in order to obtain a good comprehensive transmission performance of a hydraulic mechanical power reflux transmission [14]. Fahdzyana *et al.* have achieved the reduction in CVT variator mass, and in pulley leakage losses can be achieved without compromising performance by utilizing the benefits of simultaneous co-design integrated plant and control design framework [15], [16].

### 1.4 Previous Prototype Model

The fundamental design for the CVT proposed in this paper includes four identical slider-crank mechanisms, each of which represents one of the quadric crank chains, which are placed in parallel in the CVT. We call this CVT a linkage-type CVT (L-CVT). In most conventional CVTs, the gear ratio range is limited. One advantage of the L-CVT is that the gear ratio can be changed to infinity. In conventional belt-type CVTs, an additional hydraulic mechanism was essential to conduct the force to drive the functional parts, and this was a major cause of power loss. Several kinds of L-CVTs have different features depending on the link structure with or without additional power mechanisms.

Our first prototype model, noted in [17] has link mechanisms consisting of two sets of lever cranks, which are four-bar linkage mechanisms, arranged symmetrically. The first prototype model of the L-CVT in our previous effort had four-bar linkage mechanisms with actuators for changing the link lengths. In order to control the rotational speed ratio between the input and output shafts, each link can be expanded and contracted by the DC motors mounted on the links. By adjusting the lengths of the crank and connecting rod, which are installed on a four-bar linkage in real time, the rocking angular velocity in the output axis can be changed continuously with the rotational speed of the crank on the input side. By transmitting the driving force through an irreversible mechanism, intermittent rotational movement in only one direction around the output shaft is created. In order to compensate for the intermittent force that occurs during conduction due to the driving force in the transmission, continuous rotational movement of the output shaft must be produced by the cooperative operation of multiple lever cranks. In addition to our conventional L-CVT, noted in [18], another prototype L-CVT model has four sets of lever cranks, which are arranged in

parallel. This L-CVT makes use of a new mechanism, in which the rotational angular velocity of the output shaft can be adjusted steplessly by expanding and contracting the lever instead of changing the lengths of the crank and connecting rod.

## 2. Structure of Linkage-Type Continuously Variable Transmission with Linkage Mechanism and Three-Dimensional Cam

### 2.1 Linkage-Type Continuously Variable Transmission Equipped with Slider-Crank Mechanism

The four-bar linkage mechanism can be categorized into three types: the double-crank mechanism, lever-crank mechanism, and double-lever mechanism. Each mechanism is classified based on conditions in each link length. In addition to these classifications, a slider-crank mechanism is also included in the four-bar linkage mechanism. Many researchers have studied linkage mechanisms such as the planar four-bar linkage mechanism [19]–[22].

Gibson *et al.* have analysed the geometry of a closed-link mechanism comprising four bars with one fixed side [19]. Ogawa *et al.* have presented a numerical synthesis procedure for four-bar linkage that combines motion generation and function generation [20]. Rothenhofer *et al.* have proposed an analytical approach to the robust design of mechanisms such as four-bar linkage or a slider-crank linkage, noted in [21] in order to achieve motion and accuracy

requirements given a desired transmission ratio and allowable geometrical variations [22]. Yan *et al.* have given a new method that integrates kinematic and dynamic design with variable input speeds is introduced for the trade-off of dynamic balancing of four-bar linkages [23].

The basic structures of the closed-loop mechanism are shown in Fig. 3. Figure 3(a) shows a fundamental four-bar linkage mechanism, and this is also called a lever-crank mechanism. Figure 3(b) shows the slider-crank mechanism that falls into the category of four-bar linkage. As for the reciprocating linear motion of the link, the movement of the piston in the cylinder in the slider-crank mechanism can be regarded as a particular circular movement such that the curvature radius of the linear motion equals infinity. The rotational force generated by the grooved cam rotating around the input shaft causes reciprocating motion of the slider, like piston movement. Finally, the force transmitted to link b is converted to the rotational force of the output shaft, which functions as a crank. As a result, the motion of the crank becomes a reciprocating angular movement within a limited angle range.

The basic structure and the appearance of a unit installed in the L-CVT are shown in Fig. 4. The basic structure of the components and the physical parameters of the unit are shown in Fig. 4(a). The cam follower corresponds to slider d (piston) in the slider-crank mechanism (Fig. 3). The outline of the unit installed in the L-CVT is shown in Fig. 4(b). The three-dimensional (3-D) cam (solid cam) rotates with input shaft O. The key and the key groove

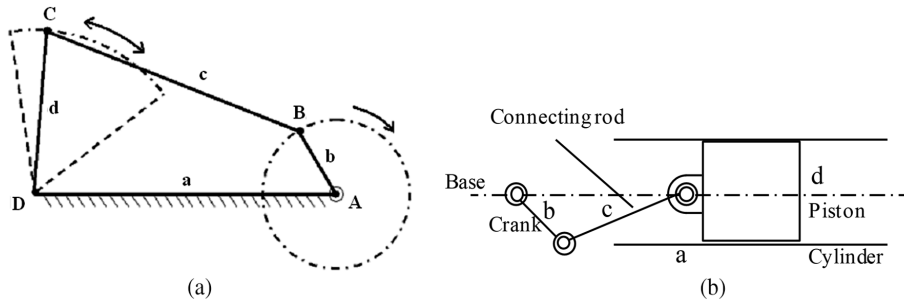


Figure 3. The fundamental structure of a closed link mechanism.

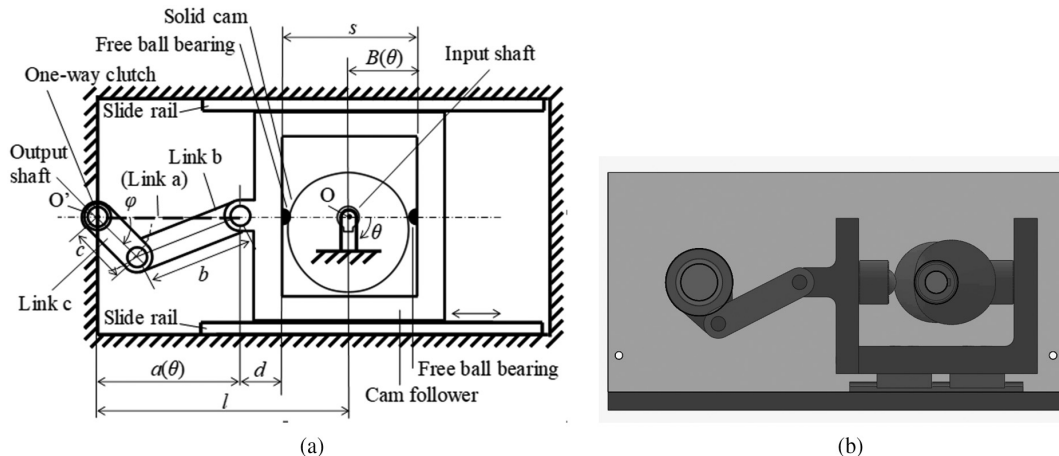


Figure 4. The unit installed in the L-CVT.

on the rotary shaft function to move the 3-D cam and the input shaft together. A couple of free ball bearings are installed on the cam follower to make contact with the 3-D cam. Thus, the 3-D cam works smoothly like a grooved cam on a 2-D plane by means of small spherical balls, regardless of their size, which are positioned on a straight line passing through the input axis O. The cam follower is subject to force from the 3-D cam rotating together with the input shaft O *via* the spherical balls, and it reciprocates on a slide rail. Each cross-sectional shape of the 3-D cam can be selected and determined independently, so that it is possible to design the gear ratio freely along the longitudinal direction of the shaft. By sliding the 3-D cam along the key groove on the input shaft in the direction along the rotation axis, stroke amount and translational speed of the cam follower can be adjusted in arbitrary gear ratios.

Next, we mention the design process for the L-CVT by dealing with only one gear ratio, as a preliminary step in designing the 3-D cam. The slider-crank mechanism, which is one of the closed chains, is composed of link b as a connecting rod, link c as a crank, and virtual link a as the reference line of the housing. The reciprocating motion of the cam follower is converted into the swing motion of link c *via* link b. Specifically, the output shaft O' rotates as a result of the difference between the rotational speeds of the inner and outer rings in the one-way clutch, and the conduction force is transmitted in only one rotation direction. All units consisting of a slider-crank mechanism that are delayed by the rotational phase of link c at equally spaced intervals are combined mechanically at both the input and output axes. Then, each generated and delayed torque in the spaced intervals is overlapped with others at the output axis. As the small spherical balls are being contacted at both side faces of the 3-D cam, the cam and the cam follower are positionally restricted. (It is possible that some rolling friction might occur). The two small spherical balls rotate in opposite directions, as the 3-D cam rotates. It follows that the 3-D cam and cam follower contacts restricted positionally can move smoothly as a secure mechanism, in which they hold a frictionless positional relationship with each other.

## 2.2 Composition of Linkage-Type Continuously Variable Transmission Unit

Here, we consider how to select the optimal number of units installed on the L-CVT. Each unit consists of a slider-crank mechanism, a 3-D cam, a cam follower, slide rails, a one-way clutch, a couple of free ball bearings, and some roller bearings, as shown in Fig. 4. Let  $n$  be the total number of units mounted on the L-CVT. The units are connected in parallel with each other in order to maintain conditions such as the specific time interval, phase lag, and rotation angles between the axes of the input and output shafts. The one-way clutch, which is an irreversible mechanism, is installed in the output shaft to restrict the rotational direction of the output shaft, and it conducts in one direction without regard to an arbitrary value  $n$ .

- (i) The case when  $n = 2$  becomes a necessary condition for a minimum value in order to realize a function as the L-CVT. The differential value with respect to the rotation angle  $\theta$  for the cam curve in the plane cam is not continuous when switching between forward and reverse rotations of the output shaft. Under the condition where an irreversible mechanism such as a one-way clutch in the freewheel is installed in the L-CVT, the cam cannot rotate smoothly. If only using the units 1 ( $n = 1$ ) and 2 ( $n = 2$ ), it is impossible to secure and maintain a section that mechanically corresponds to a rotational angle and phase in order to take over the driving of the output shaft.
- (ii) In the case of  $n = 3$ , the adjustable angular width of the non-driving section is present in every cycle for rotation of the cam at the input axis. In this case, the differential value regarding the rotation angle  $\theta$  of the cam curve corresponding to the gear ratio is not continuous at the switching point in the reciprocating movement. However, the differential value of the cam curve with regard to angle  $\theta$  can be set continuously at the moment when switching between the forward and reverse rotations of the output shaft using the curve-fitting technique. A velocity scheme of the output link in the backward path as reverse rotation can be designed with enough range inside of the non-driving section so that smooth rotation of the cam occurs. It is impossible to provide a takeover section that corresponds to a changeover period of about  $\pi/18$  and conducts a large enough force if and only if the unit 1 ( $n = 1$ ), 2 ( $n = 2$ ), or 3 ( $n = 3$ ) takes over the driving force. In this condition, it has a weak point where the slope of the cam curve is slightly steep in the range of the non-driving section.
- (iii) In the case of  $n = 4$ , the ratio of the takeover section to the driving one for only one unit is defined as the coefficient parameter  $k(0 \leq k \leq n/2 - 1)$  with respect to the takeover coefficient. The coefficient value is given by the ratio of the angular range to the driving section for one cycle in the input shaft which rotates with the cam around the rotation axis. The takeover interval then becomes  $2\pi k/n$ . Also, it is understood that the driving section needed as a design requirement for every one unit is at least  $2\pi(1+k)/n$ . Assume the number of units that can transmit the conduction force simultaneously in parallel during the takeover section to be  $n'$ . As for the number of drive paths, the conduction forces are transmitted in parallel through at least two ( $n' = 2$ ) units in the L-CVT. The conduction force and torque between each unit in the L-CVT is being distributed to every  $1/n' (= 1/2)$  at that moment. Then, the distributed torques are combined into the resultant torque at the output shaft.
- (iv) In the case of  $n \geq 5$ , the ratio of the takeover section to the driving section is increased or decreased depending on the magnitude of  $k/n$ . The drive units can be alternated in order to conduct force and torque continuously by the ratio of the sections. If  $n$  is large, the conduction force can be transmitted

through a multiple-branched transmission path by means of  $n' (> 2)$  units. Then, the transmission torque conducted between units is distributed to every  $1/n'$ . The distributed transmission force is conducted as the resultant torque at the output shaft. Thus, it is necessary to deal with the relationship between the number  $n'$  of parallel drive units and the stiffness of each link in the L-CVT as a design parameter.

### 3. Design of 3-D Cam

#### 3.1 Design of Planar Cam

As for the physical parameters shown in Fig. 2, the length  $b$  of link b (connecting rod), the length  $c$  of link c (crank), the distance  $s$  between the centres of both free spherical ball bearings, the distance  $d$  between the centre of the spherical ball on the left side and the rotation axis where link b and a cam follower are connected, and the distance  $l$  between the input and output axes which are fixed values are defined. As previously mentioned, the size of the free ball bearing installed in the L-CVT is assumed to be significantly small, and the radius  $r$  of the sphere is set to  $r = 0$  [mm]. The dimensions of the prototype L-CVT model used as the experimental equipment are  $b = 50$ ,  $c = 25$ ,  $s = 80$ ,  $d = 35$ , and  $l = 130$  [mm]. The length  $a(\theta)$  of a virtual link and a cam base curve  $B(\theta)$  in the cam diagram are variables related to the rotation angle  $\theta$  of the cam, which differs depending on the gear ratio  $R$ . The plane cam is designed so that link c rotates counter-clockwise in the section  $0 \leq \theta \leq \pi$ , while link c rotates clockwise in the section  $\pi \leq \theta \leq 2\pi$ . At this time,  $a = a(\theta)$  is set to the maximum value  $a(0) = a_{max}$  when  $\theta = 0$ , and the minimum value  $a(\pi) = a_{min}$  when  $\theta = \pi$ .

The relationship between the cam base curve  $B(\theta)$ , a cam curve  $h(\theta)$ , and the base circle radius  $r_0$  of the cam can be expressed as

$$B(\theta) = r_0 + h(\theta) \quad (1)$$

The relationship between the cam curve  $h(\theta)$  and the length  $a(\theta)$  of the virtual link is given by

$$h(\theta) = a(\theta) - a_{min} = a(\theta) - a(\pi) \quad (2)$$

Using (1) and (2), the relationship is obtained as follows:

$$r_0 = s + d - l + a_{min} = s + d - l + a(\pi) \quad (3)$$

Let the maximum value of the cam curve  $h(\theta)$  be  $h_{max}(= a_{max} - a_{min})$ . Then, we have the following equation.

$$s = 2r_0 + h_{max} \quad (4)$$

From (3) and (4), the following equation can be obtained as

$$2l - 2d - s = a_{max} + a_{min} \quad (5)$$

As the left side of (5) is invariant, and the sum of the maximum and minimum values of  $a = a(\theta)$  is constant regardless of the speed ratio ( $a_{max} + a_{min} = \text{Const.}$ ), it is

possible to satisfy a positional constraint condition in the cam design.

Next, we obtain the relationship between the rotation angle  $\theta$  of the cam fixed with the input axis and the cam base curve  $B(\theta)$ . As the cam is held by two spheres in the mechanism, it is necessary only to calculate  $B(\theta)$  in the section  $0 \leq \theta \leq \pi$  for one period, which is able to correspond to all sections of  $0 \leq \theta \leq 2\pi$ . The curve  $B(\theta)$  in the interval of  $\pi \leq \theta \leq 2\pi$  can be given by the following equation.

$$B(\theta) = s - B(\theta + \pi) \quad (6)$$

By only determining  $B(\theta)$  in the range of  $0 \leq \theta \leq \pi$ ,  $B(\theta)$  in all sections of  $0 \leq \theta \leq 2\pi$  can be obtained from (6). That is, from (1), (2), and (4),  $B(\theta)$  can be obtained using  $a(\theta)$ . The relationship between  $\theta$  and  $B(\theta)$  can also be obtained from  $\theta$  and  $a(\theta)$ . Note that the curve  $B(\theta)$  in (6) depends only upon  $\theta$ , and it does not include any variables related to the gear ratio  $R$ .

#### 3.2 Shape of Planar Cam (The Case in which the Gear Ratio is Constant)

Here, under the condition that the gear ratio is constant, we calculate the cam base curve  $B(\theta)$  for a gear ratio  $R$ . Using the parameter  $a(\theta)$ , which was calculated in the previous section, the Cartesian coordinates ( $B_x(\theta)$ ,  $B_y(\theta)$ ) of  $B(\theta)$  for rotation angle  $\theta$  of the cam at an arbitrary gear ratio  $R$  can be obtained. Transforming (4), the cam base circle radius  $r_0$  can be obtained as:

$$r_0 = \frac{s - h_{max}}{2} \quad (7)$$

Substituting  $h(\theta)$  and  $r_0$ , which are obtained from (2) and (7), into (1),  $B(\theta)$  is given. Then, the  $x$  and  $y$  coordinates, *i.e.*,  $B_x$  and  $B_y$  of  $B(\theta)$ , are defined as follows:

$$B_x(\theta) = B(\theta) \cos \theta \quad (8)$$

$$B_y(\theta) = B(\theta) \sin \theta \quad (9)$$

#### 3.3 Driving and Non-Driving Sections

In order to clarify the relationship between the rotation angle  $\theta$  at the input axis and the length  $a = a(\theta)$  of the virtual link, we first propose a method for separating a cycle between the driving section and the non-driving section. Let  $a(\theta^*)$  at  $\theta = \theta^*$  be an intermediate value between  $a_{max}$  and  $a_{min}$ , and let it be a reference value. The angle  $\theta^*$  is basically set to  $\theta^* = 2\pi/n$ . Note that  $a(\theta^*)$  is not the average or median value, but an arbitrary value between  $a_{max}$  and  $a_{min}$ . The length  $a = a(\theta)$  becomes the maximum value  $a = a(0) = a_{max}$  when  $\theta = 0$ , while the minimum value  $a = a(\pi) = a_{min}$  when  $\theta = \pi$ . In the previous section, it was mentioned that it should only be necessary to consider a design for  $0 \leq \theta \leq \pi$  in the angular range  $0 \leq \theta \leq 2\pi$  of the input rotation angle. The section  $0 \leq \theta \leq \pi$  is divided into two sections; *i.e.*, (i) the driving section and (ii) the non-driving section. Furthermore, (ii) the non-driving section can be further divided into two sections. Therefore, the entire interval of one cycle ( $0 \leq \theta \leq 2\pi$ ) can be divided into three sections. That is,

the entire period  $\theta$  of the cycle consists of a total of three sections: (i) the driving section including the intermediate value as the reference value  $\theta = \theta^*$ , and (ii) two non-driving sections. The result shows that the ratio of the section widths of (i) and (ii) becomes  $2\pi(1+k)/n: \pi - 2\pi(1+k)/n$ .

- (i) Driving section:  $\pi(1-k)/n \leq \theta \leq \pi(3+k)/n$
- (ii) Non-driving section:  $0 \leq \theta \leq \pi(1-k)/n, \pi(3+k) \leq \theta \leq \pi$

(i) The angular range for the driving section corresponds to the range of the rotation angle  $\theta$  for the input shaft in the period when the driving force is being transmitted from the link c to the output shaft *via* the irreversible mechanism. Then, the output angular velocity  $d\varphi/dt$  of link c always becomes a constant value ( $d\varphi/dt = \text{Const.}$ ) when the input angular velocity  $d\theta/dt$  is constant ( $d\theta/dt = \text{Const.}$ ) in the driving section. The output angular velocity  $d\varphi/dt$  can be obtained by dividing the input angular velocity  $d\theta/dt$  by the gear ratio  $R$ . A total of  $n(=4)$  sets of slider-crank mechanisms are used in the L-CVT. In total,  $n(=4)$  sets of 3-D cams are delayed by every phase lag  $2\pi/n$  ( $=\pi/2$ ) at constant intervals. In the previous section, we gave an example in which the number of units transmitting in parallel at the same time was  $n'(=2)$  within a total of  $n(=4)$  sets of slider-crank mechanisms installed in the L-CVT.

Here, we focus on a situation in which only one set  $n'(=1)$  of a total of  $n$ -sets of slider-crank mechanisms, which are connected in parallel at the output axis, transmits force to the output axis in parallel, simultaneously. The value of the minimum range of rotational angular displacement of the 3-D cam, which can transmit the driving force becomes  $2\pi/n$ , which is obtained from dividing one cycle by  $n$  when the takeover coefficient  $n$  is zero ( $k=0$ ). The rotational angle for transmitting the driving force is in inverse proportion to the magnitude of  $n$  under the condition that  $k$  is constant. That is, the angular displacement becomes small because the range of rotational angular displacement of the 3-D cam conducting the driving force is  $2\pi/n$  when using  $4 \leq n$  as the number of slider-crank mechanisms. The range of the swing angle becomes  $n(1-k)\Delta\varphi$  in  $n$  sets of slider-crank mechanisms when the range of the swing angle output from one set of slider-crank mechanisms equals  $\Delta\varphi$  with respect to the output angular displacement. If the number of slider-crank mechanisms is  $4 \leq n$ , the output range of the swing angle in a set of mechanisms expands in proportion to the magnitude of  $n$  under the condition that  $k$  is constant.

### 3.4 Length of Virtual Link in Driving and Non-Driving Sections

In order to obtain the relationship between the rotation angle  $\theta$  and the length  $a = a(\theta)$  of the virtual link, we consider (i) the driving section and (ii) the non-driving section independently.

#### (i) Driving section

As mentioned in the previous section, one parameter  $a(\theta)$  is determined within the angle range  $0 \leq \theta \leq \pi$ , and

the other parameter  $a(\theta + \pi)$  is determined to satisfy the structural condition of a positive cam for rotational angle  $\theta(0 \leq \theta \leq 2\pi)$  of the input shaft. Note that the whole shape of the cam over one cycle is not utilized for the driving intervals. Also, the non-driving section is included in the range ( $0 \leq \theta \leq \pi$ ) of the rotation angle of the input shaft in a similar way. Based on the value of  $a(\theta^*)$  explained in the previous section, the swing range of link c can be determined. The value of  $a(\theta^*)$  can be set as a constant so as not to depend upon any gear ratios. According to the upper design specification for the L-CVT,  $\theta^*$  as the reference point can also be changed for each gear ratio. Note that  $2a(\theta^*) \neq a(0) + a(\pi)$  is satisfied by the relationship among the actual output angular displacements  $\varphi(0)$ ,  $\varphi(\theta^*)$ , and  $\varphi(\pi)$ . Considering the conditions in the non-driving section, the takeover section, and the number of units, the inequality  $a(0) < a(\theta^*) < a(\pi)$  from the structural relationship can be satisfied using a reference value  $a(\theta^*)$ . From (5),

$$a(\theta^*) = l - d - \frac{s}{2} \quad (10)$$

is given. Using the cosine theorem, the swing angle  $\varphi(\theta)$  of link c can be obtained as:

$$\varphi(\theta) = \cos^{-1} \left\{ \frac{\{a(\theta)\}^2 + c^2 - b^2}{2ca(\theta)} \right\} \quad (11)$$

By substituting  $\theta = \theta^*$  into (11),  $\varphi(\theta^*)$  is given. The value  $a(\theta)$  in the driving section can be obtained from the value of  $\varphi(\theta^*)$ . We suppose that the speed gear ratio is  $R$  and the conditions  $n = 4$  and  $k = 1/9$  are satisfied. The output angle  $\varphi(\theta)$  of link c in the driving section ( $2\pi/9 \leq \theta \leq 7\pi/9$ ) is given by

$$\varphi(\theta) = \varphi(\theta^*) + \frac{\theta - \theta^*}{R} \quad (12)$$

In (12) gives the relationship between the input angle  $\theta$ , the output angle  $\varphi(\theta)$ , and the reduction ratio  $R$ . The value of the parameter  $a(\theta)$  in the range of the driving section can be given by substituting  $\varphi(\theta)$  obtained from (12) into the following equation:

$$a(\theta) = c \cos \varphi(\theta) - \sqrt{b^2 - c^2 \sin^2 \varphi(\theta)} \quad (13)$$

By modifying the cosine theorem (as shown in (11)) for a triangle connected by link b, link c, and a reference line that corresponds to virtual link a (as shown in Fig. 1), (13) can be obtained.

#### (ii) Non-driving section

Here, as for the cam design, the starting point and the ending point of  $a(\theta)$  in the driving section are connected by a continuous and differentiable point  $(\theta, a(\theta))$  in the Cartesian coordinate system  $(B_x(\theta), B_y(\theta))$  of the non-driving section. As the constraint conditions, the values of  $a(\theta)$  at the starting and ending points of each of the three sections, the first derivative  $da/d\theta$  for  $\theta$ , the second derivative  $d^2a/d\theta^2$ , and the third derivative  $d^3a/d\theta^3$  are used, respectively. Using these differential values, some

constraint conditions can be obtained from interpolation formula (21), which satisfies the following relations (14) to (20). As an example, assuming  $n = 4$  and  $k = 1/9$ , we consider a section within the range of  $7\pi/9 \leq \theta \leq \pi$ . Assuming  $f(\theta)$  as the interpolation curve for  $\theta$  in the section, the constraint condition becomes

$$f\left(\frac{7\pi}{9}\right) = a\left(\frac{7\pi}{9}\right) \quad (14)$$

$$\frac{df}{d\theta}\left(\frac{7\pi}{9}\right) = \frac{da}{d\theta}\left(\frac{7\pi}{9}\right) \quad (15)$$

$$\frac{df}{d\theta}(\pi) = 0 \quad (16)$$

$$\frac{d^2f}{d\theta^2}\left(\frac{7\pi}{9}\right) = \frac{d^2a}{d\theta^2}\left(\frac{7\pi}{9}\right) \quad (17)$$

$$\frac{d^2f}{d\theta^2}(\pi) = 0 \quad (18)$$

$$\frac{d^3f}{d\theta^3}\left(\frac{7\pi}{9}\right) = \frac{d^3a}{d\theta^3}\left(\frac{7\pi}{9}\right) \quad (19)$$

$$\frac{d^3f}{d\theta^3}(\pi) = 0 \quad (20)$$

From the seven conditional (14) to (20) above, the formula  $f(\theta)$  can be interpolated by expressing it as a six-order polynomial:

$$f(\theta) = A_1\theta^6 + B_1\theta^5 + C_1\theta^4 + D_1\theta^3 + E_1\theta^2 + F_1\theta + G_1 \quad (21)$$

The coefficients  $A_1, B_1, C_1, D_1, E_1, F_1,$  and  $G_1$  are calculated by substituting (14) to (20) into (21). By substituting  $\theta$  into  $f(\theta)$  obtained by (21) in the limited range of  $\theta(7\pi/9 \leq \theta \leq \pi)$ , both  $f(\theta)$  in the range and a curve that is smoothly connected with  $a(\theta)$  are obtained. The value of  $a(0) = a_{\max}$  can be given by substituting the value satisfying  $a(\pi) = a_{\min}$  into (5). Substituting the value of  $a(\pi) = a_{\min}$  into (5),  $a(0) (= a_{\max})$  is obtained.

In a similar way, we assume the conditions  $n = 4$ ,  $k = 1/9$ , and the section of  $0 \leq \theta \leq 2\pi/9$ . Defining the interpolation curve in this section as  $g(\theta)$ , the constraint conditions are as follows:

$$g(0) = a(0) \quad (22)$$

$$g\left(\frac{2\pi}{9}\right) = a\left(\frac{2\pi}{9}\right) \quad (23)$$

$$\frac{dg}{d\theta}(0) = 0 \quad (24)$$

$$\frac{dg}{d\theta}\left(\frac{2\pi}{9}\right) = \frac{da}{d\theta}\left(\frac{2\pi}{9}\right) \quad (25)$$

$$\frac{d^2g}{d\theta^2}(0) = 0 \quad (26)$$

$$\frac{d^2g}{d\theta^2}\left(\frac{2\pi}{9}\right) = \frac{d^2a}{d\theta^2}\left(\frac{2\pi}{9}\right) \quad (27)$$

$$\frac{d^3g}{d\theta^3}(0) = 0 \quad (28)$$

$$\frac{d^3g}{d\theta^3}\left(\frac{2\pi}{9}\right) = \frac{d^3a}{d\theta^3}\left(\frac{2\pi}{9}\right) \quad (29)$$

From the upper eight conditional (22) to (29),  $g(\theta)$  is interpolated by expressing it as a seven-order polynomial as follows:

$$g(\theta) = A_2\theta^7 + B_2\theta^6 + C_2\theta^5 + D_2\theta^4 + E_2\theta^3 + F_2\theta^2 + G_2\theta + H_2 \quad (30)$$

The coefficients  $A_2, B_2, C_2, D_2, E_2, F_2, G_2,$  and  $H_2$  are calculated by substituting (22) to (29) into (30). Specifically, by substituting  $\theta$  into  $g(\theta)$  obtained by (30) in the limited range of  $\theta(0 \leq \theta \leq 2\pi/9)$ ,  $g(\theta)$  within this section and a curve that is smoothly connected with  $a(\theta)$  can be obtained.

(iii) From (i) and (ii) above,  $f(\theta)$  and  $g(\theta)$ , which are smoothly connected to  $a(\theta)$ , are obtained in the range  $0 \leq \theta \leq \pi$ . Transforming (6) using (1), (2), and (4), the relationship is given as

$$a(\theta) = a_{\max} + a_{\min} - a(\theta - \pi) \quad (31)$$

Furthermore, by substituting  $\theta$  into (31) in the limited range ( $\pi \leq \theta \leq 2\pi$ ),  $a(\theta)$  within the range can be obtained. The rotational angular velocity of the input shaft is set to  $2\pi$  [rad/s]. As four sets of cams and link mechanisms are used in this design, the phase range of the output shaft, in which one set of mechanisms outputs the driving force equals to  $90$  [°]. It is possible that the force applied to the output shaft is interrupted for a moment due to backlash in the one-way clutch, or errors in processing and assembly if the output drive section is set to just  $90$  [°]. To overcome this problem, the parallel conduction while two sets of units output the driving force cooperatively in the takeover section within the range of  $\pm 5$  [°] of the phase at the moment when the driving unit is switched is designed. The takeover section prevents the force from being constantly interrupted to the output shaft. Therefore, it becomes interval corresponding to total angle of  $100$  [°] in which the driving force is output by the output link installed in one set of units. On the other hand, the interpolation interval is for smoothly connecting the output interval for driving force transmission and the interval of  $\pi \leq \theta \leq 2\pi$ . Figure 5 shows the phase angles of the drive section and the interpolation section. Figure 6 shows the time response of  $a(\theta)$  when the gear ratio is 3, 5, 10, or  $\infty$ . Thus,  $a(\theta)$  in the whole interval  $0 \leq \theta \leq 2\pi$  can be obtained. In terms of the first derivative  $d\varphi/dt$  for  $t$ , Fig. 7 shows the responses of angular velocity  $d\varphi/dt$  of link  $c$ . Also, the following relationships can be satisfied with regard to  $f(\theta)$  and  $g(\theta)$ .

$$f(\theta) = a_{\max} + a_{\min} - f(\theta - \pi) \quad (32)$$

$$g(\theta) = a_{\max} + a_{\min} - g(\theta - \pi) \quad (33)$$

Next, substituting the obtained  $a(\theta)$  into (11), the angle  $\varphi(\theta)$  of link  $c$  is calculated. Substituting  $a(\theta)$  into (11), the angle  $\varphi(\theta)$  of link  $c$  is derived. Furthermore, by differentiating  $\varphi(\theta)$  with respect to time  $t$ , the angular velocity  $d\varphi/dt$  of the swing motion of link  $c$  is obtained.

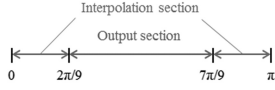


Figure 5. An output section and interpolation sections.

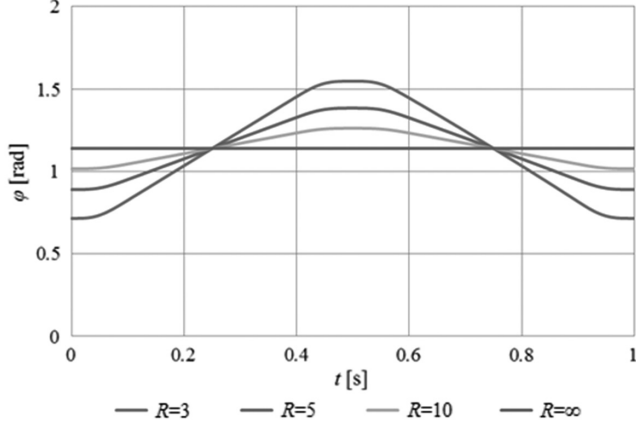


Figure 6. Responses of angle  $\varphi$  of link c.

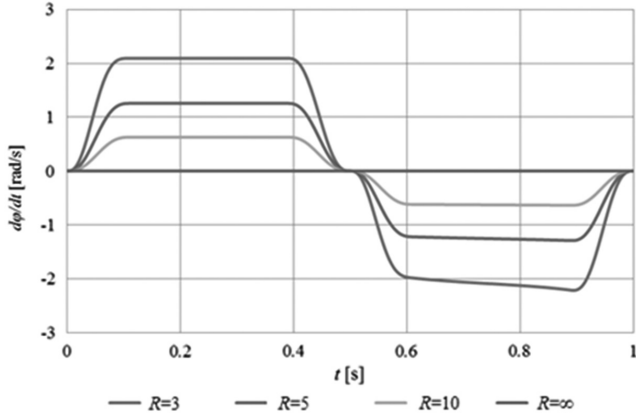


Figure 7. Responses of angle  $d\varphi/dt$  of link c.

### 3.5 Shape of 3-D Cam

In order to design the shape of the 3-D cam, we define the Cartesian coordinate system  $(B_x, B_y, B_z)$  of the 3-D cam passing through the centre coordinates of the spherical ball installed in the free ball bearing. In terms of the arbitrary gear ratio  $R$  and the rotation angle  $\theta$  of the cam,  $B_x$  and  $B_y$  of the cam curve  $B(\theta)$  can be obtained using (8) and (9) from the previous section.  $B_z$  stands for the coordinate in the direction along the rotation axis of the 3-D cam. As there is no correlation between the sectional shape  $(B_x(\theta), B_y(\theta))$  of the 3-D cam and the gear ratio  $R$ , the parameter  $B_z$  in the longitudinal direction for each gear ratio  $R$  along the rotating shaft can be designed freely using another variable according to range in the distance. The length in the longitudinal direction in the 3-D cam increases the whole size of the L-CVT device. Although the 3-D inclination in the 3-D cam becomes relatively steep for the decision of  $B_z$ , the L-CVT apparatus is downsized if the distance in the longitudinal direction along the

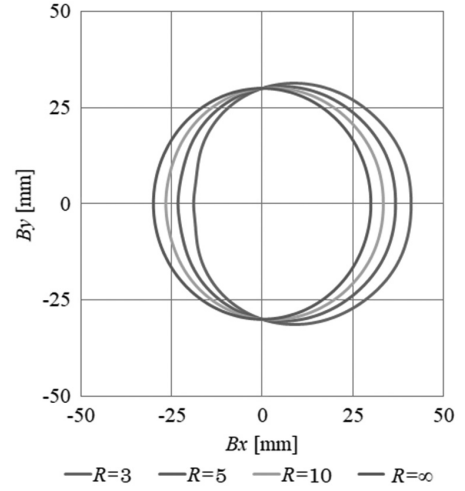


Figure 8. External shapes of flat cams created based on the cam diagram corresponding to each gear ratio.

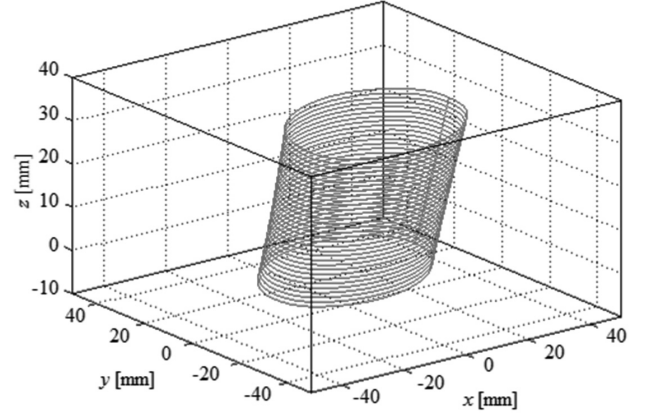


Figure 9. The shape of the 3-D cam.

rotation axis is shortened. The gentle curve in the 3-D cam facilitates the shifting of gears when sliding along the axial direction. Figure 8 shows external shapes of flat cams created based on the cam diagram corresponding to each gear ratio. The figure stands for the relationship between  $B_x$  and  $B_y$ , and the  $B_x$ - $B_y$  curve represents a sectional view of the 3-D cam. The figure shows curves for four gear ratios  $R = 3, 5, 10$ , and infinity. The  $B_x$ - $B_y$  curves become a circle that is centred on the input rotation axis  $O$  ( $B_x = B_y = 0$ ) when the gear ratio  $R$  equals infinity. Figure 10 shows the outline view of the designed 3-D cam using 3-D CAD software. The 3-D cam can be obtained by taking the variable of the gear ratio along the rotation axis direction and by superimposing the cam displacement curves at each gear ratio obtained in Figs. 8 and 9. The cam and the rotating shaft are integrated by a shaft with a key groove.

### 4. Conclusion

We have proposed a CVT which is composed of closed-loop linkages, cams, and non-invertible mechanisms. A CVT consisting of slider-crank linkages, the three-dimensional

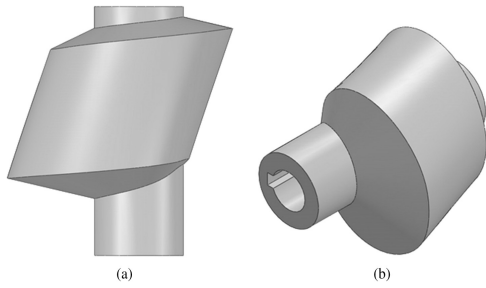


Figure 10. The outline view of the designed 3-D cam using 3-D CAD software.

cams, and one-way clutches was discussed in this paper. As the basic structure of the L-CVT, multiple units were connected in parallel, and the geometric relationship of each element in each unit was derived. We have considered the optimal number of units installed in the L-CVT. It was understood about the necessity of considering the number of parallel drive units as one of the design parameter of the L-CVT. Also, we have defined that the coordinates to shape the flat plate cam in the case in which the reduction gear ratio was constant. Also, the driving and non-driving sections in order to clarify the relationship between the rotation angle at the input axis and the length of the virtual link was defined. Next, we have designed a mechanism consisting of conduction units installed in the L-CVT, in which a total of four units composed of a slider-crank unit with a link mechanism that is expanded and contracted by means of a 3-D cam are arranged in parallel. The 3-D cam suppresses the frictional force, and it conducts the force and torque smoothly to the output shaft, unlike in conventional CVTs, which have another mechanism such as a planetary gear. Four units were mechanically connected in parallel with the cranks at the input shaft and mechanically with the output shaft *via* four sets of irreversible mechanisms such as one-way clutches installed at the fulcrum of each lever. Finally, we performed several analyses that confirmed the effectiveness of the L-CVT, as it was shown that the gear ratio could be controlled continuously by realizing a 3-D cam. As the L-CVT is not composed of frictional conduction mechanism, it provides several performances that creates no noise, is durable, and offers high transmission efficiency. In the future work, we will assemble the prototype machine of the L-CVT and evaluate the power consumption of the developed L-CVT.

## References

- [1] X. Shi, Q. Gao, W. Li, and H. Guo, Simulation and experimental study on gear fault diagnosis simulation test bench of wind generator, *Journal of Mechatronic Systems and Control*, 47(1), 2019, DOI: 10.2316/J.2019.201-2963.
- [2] J. Si, Y. Cao, and X. Shi, Fault diagnosis of wind turbine planetary gearbox based on HHT and structure resonance demodulation, *Journal of Mechatronic Systems and Control*, 47(1), 2019, DOI: 10.2316/J.2019.201-2966.
- [3] E. Boufounas and A. Amrani, Optimal multivariable control for wind energy conversion systems using particle swarm optimization technique, *Journal of Mechatronic Systems and Control*, 45(4), 2017, DOI: 10.2316/Journal.201.2017.4.201-2865.
- [4] Z. Farnaz, H.S. Sajith, A.D. Abeysekara, S. Welikala, P.J. Binduhewa, P.B. Ekanayake, and L. Samaranayake, DC motor torque control using state estimation, *Journal of Mechatronic Systems and Control*, 44(3), 2016, 130–138, DOI: 10.2316/Journal.201.2016.3.201-2762.
- [5] D. Rockwood, N. Parks, and D. Garmire, A continuously variable transmission for efficient urban transportation, *Sustainable Materials and Technologies*, 1–2, 2014, 36–41.
- [6] Y. Itoh and T. Sakaguchi, Development of the mono ring CVT, *NTN Technical Review*, 73, 2005, 60–65.
- [7] S. Miyata and D. Liu, Study of the control mechanism of a half-toroidal CVT during load transmission, *Journal of Advanced Mechanical Design, Systems, and Manufacturing*, 1(3), 2007, 346–357.
- [8] J. Ingvast, J. Wikander and C. Ridderstrom, The PVT, an elastic conservative transmission, *The International Journal of Robotics Research*, 25(10), 2006, 1013–1032.
- [9] J. Kim, F.C. Park, and Y. Park, Design, analysis and control of a wheeled mobile robot with a nonholonomic spherical CVT, *International Journal of Robotics Research*, 21(5), 2002, 409–426.
- [10] A. Afrabandpey and H. Ghariblu, Performance evaluation of ball CVT and comparison with half toroidal CVT, *International Journal of Automotive Technology*, 19(3), 2018, 547–557.
- [11] B. Pohl, M. Simister, R. Smithson, and D. Miller, Configuration analysis of a spherical traction drive CVT/IVT, *SAE Int.*, 2004, 2004-40-0009.
- [12] J.T. Belter and A.M. Dollar, A passively adaptive rotary-to-linear continuously variable transmission, *IEEE Transactions on Robotics*, 30(5), 2014, 1148–1160.
- [13] Z.B. Saribay and R.C. Bill, Design analysis of pericyclic mechanical transmission system, *Journal Mechanism and Machine Theory*, 61, 2013, 102–122.
- [14] Y. You, D. Sun, D. Qin, B. Wu, and J. Feng, A new continuously variable transmission system parameters matching and optimization based on wheel loader, *Mechanism and Machine Theory*, 150, 2020, 103876.
- [15] C.A. Fahdzyana, S. van Raemdonck, K. Vergote, and T. Hofman, Joined plant and control design for continuous variable transmission systems, *American Control Conf. (ACC)*, 2020.
- [16] C.A. Fahdzyana, M. Sakazar and T. Hofman, Integrated plant and control design of a continuously variable transmission, *IEEE Transactions on Vehicular Technology*, 70(5), 2021, 4212–4224.
- [17] T. Yukawa, T. Kumada & G. Obinata, Continuously variable transmission using quadric crank chains, *8th IEEE International Conference on Industrial Informatics (INDIN 2010)*, 2010, 1043–1048.
- [18] T. Yukawa, Continuously variable transmission using quadric crank chains and ratchets, *Proceedings of International Conference on Renewable Energies and Power Quality (ICREPQ 2011)*, 2011, 264.
- [19] C.G. Gibson and P.E. Newstead, On the geometry of the planar 4-bar mechanism, *Acta Applicandae Mathematica*, 7, 1986, 113–135.
- [20] K. Ogawa and Y. Yokoyama, Synthesis of the planar four-bar linkage, *The Japan Society of Mechanical Engineers (JSME) Bulletin of JSME*, 12(54), 1969, 1503–1511.
- [21] A. Nagchaudhuri, Mechatronic redesign of slider crank mechanism, *Proceedings of IMECE 2002*, 2002, 1–6.
- [22] G. Rothenhofer, C. Walsh, and A. Slocum, Transmission ratio based analysis and robust design of mechanisms, *Precision Engineering*, 34(4), 2010, 790–797.
- [23] H.S. Yan and R.C. Soong, Kinematic and dynamic design of four-bar linkages by links counterweighing with variable input speed, *Mechanism and Machine Theory*, 36, 2001, 1051–1071.

## Biographies



*Toshihiro Yukawa* He is currently an associate professor at Iwate University in Japan. He received the Ph.D in mechanical engineering from Tohoku University, Japan, in 1996.